- Technical Report -

APPARENT COEFFICIENT OF THERMAL EXPANSION FOR EVALUATING VOLUME CHANGES OF EARLY-AGE CONCRETE

Di QIAO[*1], Akiko OGAWA[*2], Masaro KOJIMA[*3], and Daijiro TSUJI[*4]

ABSTRACT

Both laboratory and in-situ tests were carried out using normal concrete (NC) and the one having a high amount of ground granulated blast furnace slag in the binder (BC) to study the evolution of apparent coefficient of thermal expansion (CTE), which yielded a three-stage development for early-age concrete. The laboratory test showed that NC had similar apparent CTEs at stage II and III due to insignificant variation of internal relative humidity (RH), while BC had a further drop at stage III related to a pronounced RH reduction. The in-situ test showed more deviation in NC than in BC.

Keywords: apparent coefficient of thermal expansion, ground granulated blast furnace slag, thermal and autogenous deformation, relative humidity

1. INTRODUCTION

Proper prediction of early-age volume changes of concrete in the design process is of great importance for reducing thermal cracking risk of mass concrete. The development of early-age stress is driven by thermal expansion and autogenous deformation. To understand the relative importance of these two mechanisms and describe each deformation for stress calculation, a number of studies [1-3] focused on separation of thermal and autogenous strains and the determination of coefficient of thermal expansion (CTE). The experimental techniques proposed, however, are not suitable for field situations as they require applications of thermal pulses to the temperature history [1, 2] or special testing apparatus [3]. Since the total deformation, i.e. the sum of thermal and autogenous deformation, can be easily and accurately measured in the field, the use of the derived apparent CTE would be helpful for engineering practices.

This report presents a comparison of laboratory and in-situ tests on the apparent CTE of early-age concrete. The variations of internal temperature and relative humidity (RH) and the development of total strain in concrete were examined in these tests.

This study also includes both normal concrete made with ordinary Portland cement (OPC) and a type of low-carbon concrete having a high amount of ground granulated blast furnace slag (GGBFS) in the binder. The use of GGBFS can contribute to controlling the temperature in mass concrete. Such concrete, however, was reported to have higher thermal expansion and autogenous deformation than normal concrete [2]. More attention should be paid.

2. TEST PROGRAMS

2.1 Test series and specimen dimension

Table 1 shows a summary of the test series, in which NC denotes normal concrete, while BC stands for the one with a high amount of GGBFS (64.5% of the binder). The laboratory test used 200mm long cylindrical specimens with a diameter of 100mm as shown in Fig.1. For each series, two replicate cylinders were used for monitoring the development of internal strain and the RH variation, respectively.

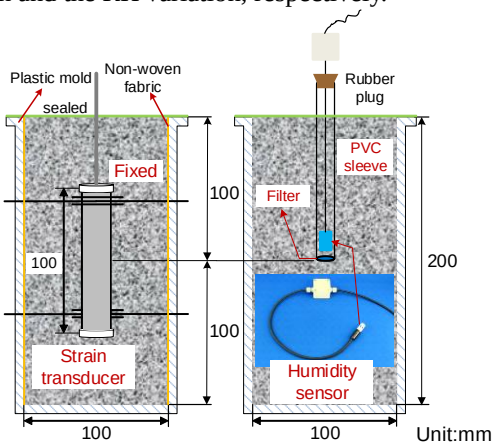

Fig.1 Laboratory test conditions

The cylindrical specimens with their molds unremoved were placed in a temperature controlled water bath, and subjected to a temperature history elevated up to 60˚C, which simulated the hydration heat induced temperature history in mass concrete. Specifically, the temperature was kept as 20˚C for the first eight hours and increased up to 60˚C within the following 16h with a temperature increasing rate of

*1 Researcher, Structural Materials Group, Takenaka Research & Development Institute, Dr.E., JCI Member
*2 Researcher, Takenaka Research & Development Institute, M.E., JCI Member
*3 Group Leader, Takenaka Research & Development Institute, Doctoral candidate, JCI Member
*4 Chief Researcher, Takenaka Research & Development Institute, Doctoral candidate, JCI Member

Table 1 Test series

Test locations	Test series	Concrete	Specimen	Edge length (mm)	Curing scheme
Laboratory	NC-1-W	NC-1	cylinders	ϕ100×200	60˚C water curing
	NC-1-S				60˚C sealed curing
	BC-1-W	BC-1			60˚C water curing
	BC-1-S				60˚C sealed curing
In situ (RMC plant, Tokyo)	NC-2-length	NC-2	cubes	1000, 400	semi-adiabatic curing
	NC-2-C		cylinders	ϕ100×200	
	BC-2-length	BC-2	cubes	1000, 800, 600, 400	
	BC-2-C		cylinders	ϕ100×200	

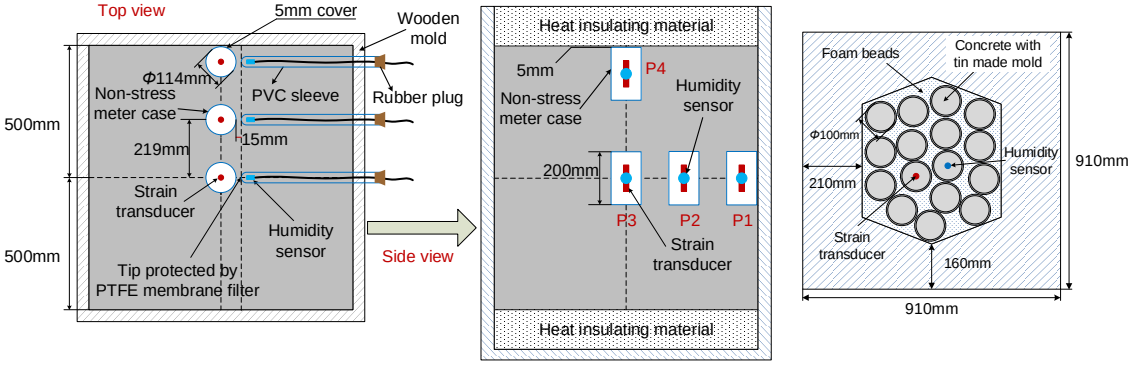

Fig.2 In-situ test conditions

2.5˚C/h. The highest temperature was kept for 12h and then the specimens were cooled to 20˚C until the age of seven days. To study the possible effect of moisture content on the apparent CTE, two test cases with or without exchange of water with the bath were carried out using a pervious plastic mold (non-stress meter case; TML) and a normal one (plastic), respectively.

For the in-situ test, both cubic concrete members with varied edge lengths and cylindrical specimens were examined under semi-adiabatic curing conditions. The cubic specimens were cast using wooden molds, of which the top and bottom sides were thermally insulated using polystyrene foam of 150mm thick to minimize the heat exchange with air as shown in Fig.2. On the other hand, the cylinders prepared with the tin made molds were stored in a simple insulated tank made of polystyrene foam together with other specimens designed for strength tests. The molds remained unremoved during the whole testing process.

2.2 Materials

The characteristics of materials used for casting NC and BC are shown in Table 2. For BC, the ordinary Portland cement (OPC) was largely substituted with a compound of GGBFS, gypsum, and limestone powder. Table 3 presents the mix proportions of the concrete, in which the water to binder ratio (W/B) was 0.45 for all test cases. For the laboratory test, the concrete was made using a double shaft forced mixer under a room temperature of 20˚C, while the specimens of the in-situ test were cast using ready-mix concrete under an ambient temperature of about 27˚C. All the test data were recorded from the time when the casting was completed.

Table 2 Characteristics of materials

Materials	Symbol	Properties / specific gravity (g/cm^3)
Cement	OPC	3.16
Slag powder	GGBFS	2.21
Gypsum powder	Cs	2.91
Limestone powder	Cc	2.71
Sand	S1	Land sand-Mandano, Chiba / 2.60 (SSD)
	S2	Crushed sand-Senbacho, Tochigi / 2.66 (SSD)
Coarse aggregate	G1	Crushed limestone-Senbacho, Tochigi / 2.70 (SSD)
	G2	Crushed limestone-Yokoze, Saitama / 2.70 (SSD)
Water reducing agent	AE	Polycarboxylate-type / 1.01~1.13

2.3 Measuring internal temperature, strains, and RH in hardening concrete

Strain transducers (KM-100BT; TML) with an effective gauge length of 100mm were installed at the center of the cylindrical specimens (see Fig.1). These transducers also had built-in thermocouple sensors, which enabled measurements of temperature ranging from -20˚C to 80˚C. To alleviate the friction between the concrete and the mold, a single layer of non-woven fabric was glued onto the inner surface of the plastic mold, while for the tin made molds used in the in-situ test a PTFE sheet of 0.1mm thick was employed. In

Table 3 Mix proportions of concrete

Type	W/B (%)	Water (kg/m^3)	Binder (kg/m^3)		Sand (kg/m^3)		Aggregates (kg/m^3)		AE (%. b)	Target slump (cm)	Target air (%)
			OPC	Compound of GGBFS, Cs, and Cc	S1	S2	G1	G2			
NC-1	45.0	175	389	-	393	393	481	481	1.1	15.0±1.5	4.5±1.0
BC-1		171	122	258	393	393	481	481	1.1	15.0±1.5	4.5±1.0
NC-2		189	420	-	409	273	1010	-	1.0	18.0	4.5
BC-2		180	128	272	481	321	905	-	1.0	18.0	4.5

addition, for the cubic specimens, the non-stress cases with embedded strain transducers were adopted as shown in Fig.2. It is worth mentioning that the strains measured in such tests consist of both thermal and autogenous strains.

To measure the variation of RH in concrete since casting, a polymer thin-film capacitive humidity sensor (TI-A; TOPLAS) with a measurement range from 0.0% to 100.0% was employed. The humidity sensor had claimed accuracies of ±2.0% for the range of 10.0% to 90.0% and ±3.0% for the extra measurement range. Moreover, a thin-film platinum resistance thermometer sensor was also incorporated, having a similar measurement range of temperature as the strain transducer. The measuring was performed within a localized hole in the concrete created by a hollow PVC sleeve with a diameter of 15mm (see Fig.1 and Fig.2), which was placed in the mold prior to the casting. The end of the sleeve extending the specimen was sealed by a rubber plug, while the other end in contact with concrete was applied with a hydrophobic PTFE membrane filter with a pore size of 0.2μm to protect the sensor from fresh concrete, which was impermeable to liquid water but permeable to vapor. It was assumed that the environment within such a sleeve, where the RH readings were taken, was in hygrothermal equilibrium with the concrete in contact [4]. In the laboratory test, the filter was attached to the sleeve by using self-adhesive tape made of butyl rubber, which was later found likely to affect the long-term RH readings due to the release of organic gases. This influence will be described in detail in the following section. In the in-situ test, the sensor tip was secured using an O-ring and the filter was fixed with a cable gland instead, to avoid the aforementioned undesired influence.

Table 4 Measuring positions in cubic specimens

Test series	Edge length (mm)	Measuring positions			
		P1 (near surface)	P2	P3 (center)	P4 (top)
NC-2	1000	o	o	o	o
	400	o	×	o	×
BC-2	1000	o	o	o	o
	800	o	o	o	×
	600	o	×	o	×
	400	o	×	o	×

For the laboratory test, the measuring interval was one minute. On the other hand, various positions within the cubic specimens were considered to investigate the influences of specimen size and moisture redistribution. The time interval of the measurements was set to ten minutes for long-term testing. Table 4 shows a summary of the measuring positions, which are also illustrated in Fig.2.

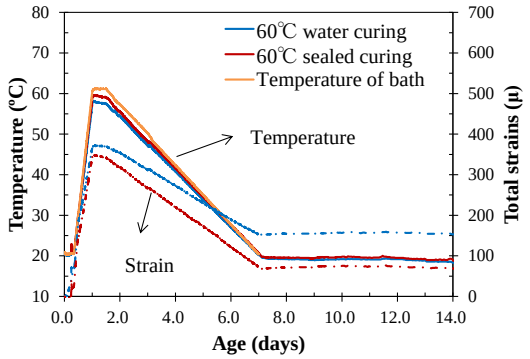

(a) NC-1

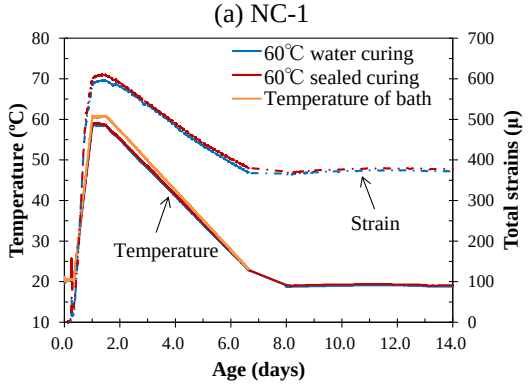

(b) BC-1

Fig.3 Temperature history and strain development

3. TEST RESULTS AND DISCUSSION

3.1 Laboratory test

Fig.3 shows the temperature histories and the strain development measured in NC-1 and BC-1. These temperatures were highly similar to those measured by the humidity sensors. Although the temperature variations at the center of the concrete followed that of the bath, the highest temperature was about 1.2˚C lower than the targeted one, likely caused by a relatively large specimen size. The strain evolution appears to be similar to that of temperature. At 14days expansion strains were found in both NC-1 and BC-1; a larger strain in BC-1 could be attributed to a higher content of SO_3 in the binder (4.04%) producing more ettringite.

As for the RH variation, the accuracy of the measurements could be improved by calibrating the sensors before and after the test with saturated salt solutions [4, 5]. Therefore, the humidity sensors were extracted from the concrete specimens and confirmed with a saturated sodium bromide solution with equilibrium RH of 59.2% (19.5˚C) at the age of about 50days. The sleeve with the filter fixed with the self-adhesive tape was employed as well. Fig.4 shows the RH readings in the created environment. It appears that the readings at the first ten hours were obviously smaller than the theoretical one; such RH output shift (-2.5% ~ -5.3%) was beyond the error range (±2.0%). Moreover, the readings were found to decrease linearly with time thereafter. It was later found out that the sensors could have been contaminated by organic gases released by the tape, which might have affected the humidity adsorbing ability of the polymer, since a new sensor without the tape yielded accurate and stable readings compared with that with tape. This influence, however, was reversible as a heat treatment with 100˚C lasting 1.5h recovered the trueness of the contaminated sensors.

Although the ambient RH of the saturated salt solution used was clearly smaller than that in the concrete, Granja *et al*. [4] found that the RH shifts were commensurate with each other across all levels of RH, showing that the linearity of the sensor response was unchanged. Given that the decreasing rate of the RH readings in the two environments was similar, it might take mere 5.5days in BC-1-S to reach the reading shift of -5.6%, compared with factory specification. Therefore, this influence could be small during the first seven days since casting. Additionally, the applied temperature history with the highest value of 60˚C might help to alleviate the influence.

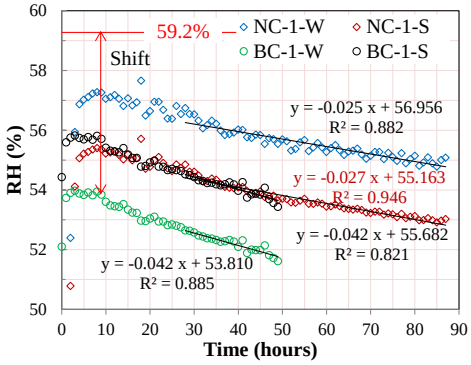

Fig.4 Calibration results using saturated sodium bromide solution

Fig.5 shows the variation of RH measured in NC-1 and BC-1 without any modifications. The RH readings of BC-1-W were partly discarded as they exceeded the measurement limit (103.0%), probably due to moisture condensation in the sleeve. It appears that RH reached a peak around 0.52days in both NC-1 and BC-1. After that, the RH in NC-1 dropped a little and then maintained, while in BC-1-S a pronounced RH drop was observed.

3.2 In-situ test

Fig.6 shows the variations of the temperatures and strains measured in the in-situ test. The RH data are not included herein because the test is still in progress and the data may need calibration.

For the cubic specimens, the highest temperature was observed at the center of the 1000mm long specimens (P3), 66.5˚C for NC-2-1000 and 58.3˚C for BC-2-1000. Their temperature differences compared with the surface (P1) were 9.1˚C and 5.7˚C, respectively. The temperature variation reached

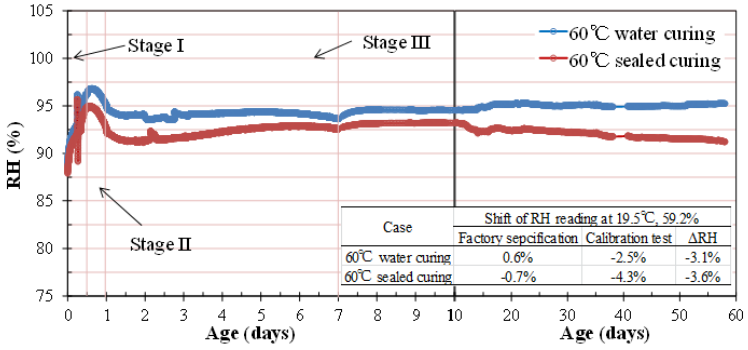

(a) NC-1

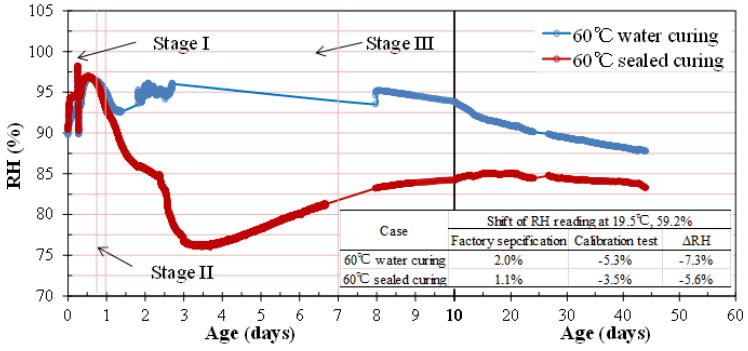

(b) BC-1

Fig.5 RH variation

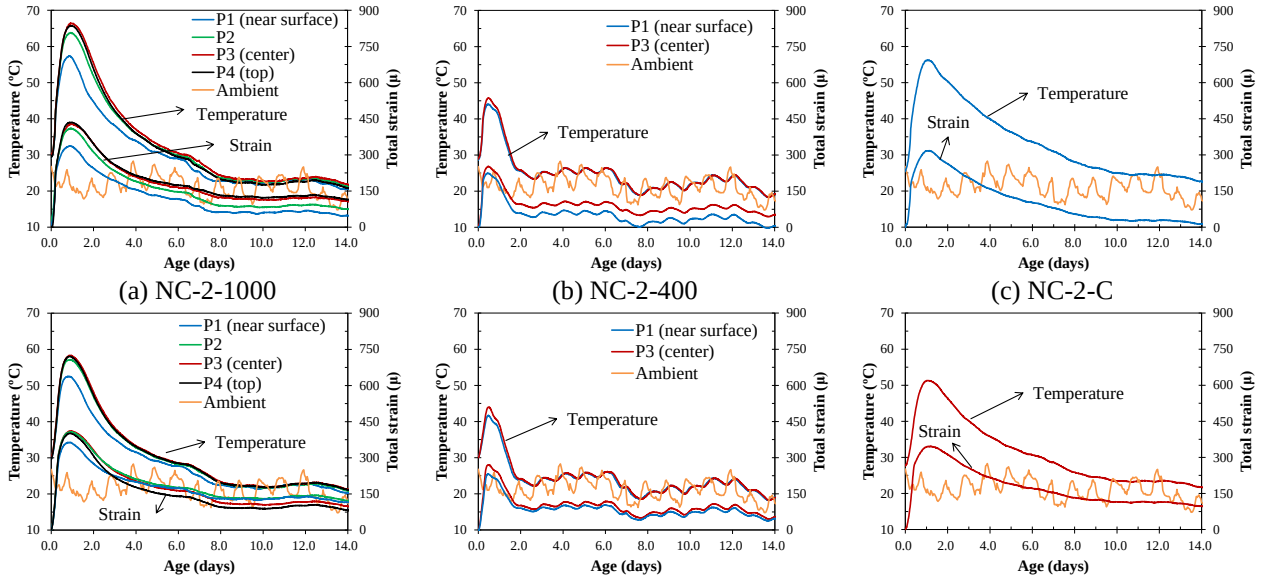

(a) NC-2-1000 (b) NC-2-400 (c) NC-2-C

(d) BC-2-1000 (e) BC-2-400 (f) BC-2-C

Fig.6 Comparison of temperature history and strain evolution between different sized specimens

equilibrium with the ambient environment after around eight days for the large cubic specimens (1000 and 800mm), while this progress was significantly shortened for smaller ones. For the cylindrical specimens, the behavior was found similar to that of P1 in the 1000mm long specimens.

As for the strain evolution, it appears that within NC-2 the strains at different positions developed in parallel. In the cooling phase, P1 had a similar reduction of strain to that of P3 under a rather smaller decrease of temperature. On the other hand, the strain development in BC-2 seems to be in proportion to the amount of temperature rise and decrease.

3.3 Apparent CTE

The apparent CTE was decided as the slope of the temperature-strain curve as shown in Fig.7, in which the data until the age of seven days were considered. A clear three-stage variation of apparent CTE, including two stages in the phase of temperature rise and one in the cooling phase, was found in most of the test cases except BC-2-400, which had the missing of stage II due to lower temperature peaks, 41.7˚C at P1 and 44.0˚C at P3.

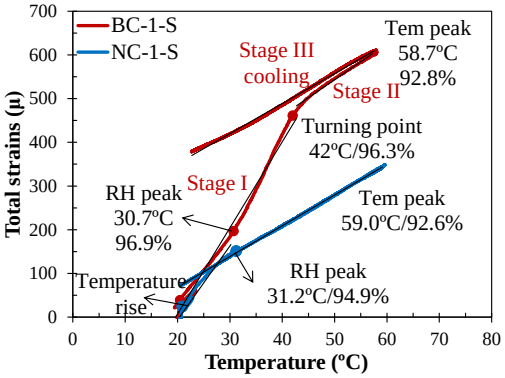

Fig.7 Example of calculation of apparent CTE

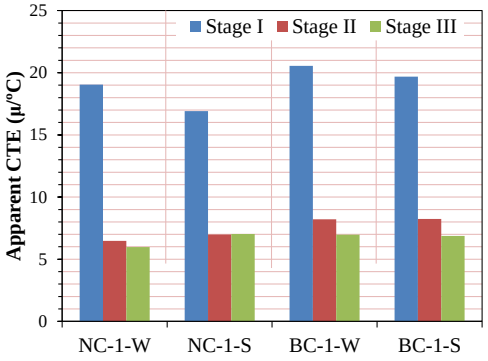

Fig.8 Apparent CTE found in laboratory test

Fig.8 shows the comparison of apparent CTE between NC-1 and BC-1. They both yielded the largest apparent CTE at stage I, which dropped to 6~8μ/˚C at stage II and III.

For NC-1, the apparent CTEs at the two later stages were similar; the difference was smaller than 0.5μ/˚C. This could be attributed to insignificant variations of RH as shown in Fig.5 (a). Such RH evolution suggests minor autogenous deformation resulting from self-desiccation, which is in agreement with the previous research [6] indicating that the effect of autogenous deformation becomes almost negligible when the W/B is greater than 0.42. On the other hand, the studies on the true CTE of cement-based materials [1-3] have shown an age-dependent behavior, i.e. the CTE initially drops as solids forms and then increases as self-desiccation proceeds, although there is a controversy concerning the time when CTE drops. Nonetheless, as the self-desiccation in NC-1 was insignificant at stage II and III, they could have negligible autogenous strain and similar true CTEs, leading to similar apparent CTEs. In comparison, for BC-1 the apparent CTE at stage III had a further drop (>1.2μ/˚C). This could be related to the pronounced RH decrease found in BC-1-S as shown in Fig.5 (b), which likely accompanied autogenous expansion even in stage

III. Maruyama and Teramoto [2] observed such expansion with the cement paste having a W/B of 0.55 and with 30% or 45% OPC replaced by GGBFS.

In addition, it appears that the higher RH observed in NC-1-W resulted in a larger apparent CTE at stage I and smaller ones at the later stages, compared with those of NC-1-S. Hence in NC-2 the larger apparent CTE at stage III (cooling) found for the surface (P1) could be related to smaller RH than that of the concrete center (P3) resulting from the lower historic temperature. The preliminary RH data of the in-situ test confirmed this point. In comparison, for BC-1 no clear connection with RH could be found except stage I. This is in consistent with BC-2, which showed similar apparent CTEs at different positions within the concrete for stage II and III.

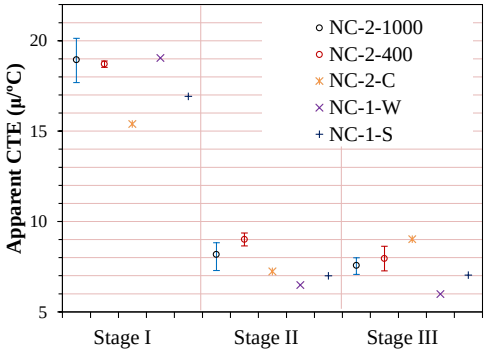

(a) NC

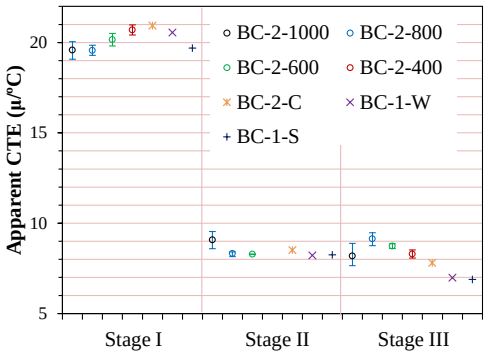

(b) BC

Fig.9 Comparison of apparent CTE between laboratory and in-situ tests

Fig. 9 shows the comparison of the calculated apparent CTEs between the laboratory and in-situ tests, in which the average value for each cubic specimen is presented with an error bar showing both maximum and minimum values obtained. Compared with BC, NC showed greater deviation within the cubic specimens and between the specimens of different sizes as well. Considering insignificant self-desiccation found in NC-1, such deviation could result from varied RH and potential moisture redistribution. This effect needs further examination based on RH data. On the other hand, the apparent CTEs of BC showed better agreement, 20.0±0.9μ/˚C for stage I and 8.6±0.9μ/˚C for stage II and III. However, the further drop at stage III found in the laboratory test was not clear in the large specimens of the in-situ test.

4. CONCLUSIONS

This study conducted both laboratory and in-situ tests to investigate the apparent CTE of early-age concrete made with OPC and the binder having a high volume of GGBFS (64.5%), respectively. The W/B was 0.45. The following conclusions can be derived:

(1) A three-stage variation of apparent CTE was found for both types of concrete. Stage I had the highest value of around 20μ/˚C; at stage II and III (cooling) it dropped to 6~9μ/˚C.

(2) For NC, the laboratory test results showed similar apparent CTE for stage II and III, which could be explained by insignificant variation of RH observed. The results also suggested a strong relation with RH value, which may cause the great deviation of the apparent CTE observed in the large specimens of the in-situ test.

(3) For BC, a further drop of the apparent CTE at stage III was noticed in the laboratory test, corresponding to the obvious RH reduction. This trend, however, was not found in the large specimens of the in-situ test. The apparent CTEs obtained within the cubic specimens and between the specimens of different sizes showed better agreement than those of NC.

ACKNOWLEDGEMENT

This work was supported by JSPS Grants-in-Aid for Scientific Research B (15H04084). The authors would like to thank Prof. Toshiaki MIZOBUCHI and Dr. Kiyoshi KOIBUCHI, Hosei University, and Dr. Tetsushi KANDA, Kajima Technical Research Institute, for their valuable comments.

REFERENCES

[1] Bjøntegaard, Ø.," Interaction between thermal dilation and autogenous deformation in high performance concrete," Mater. Struct., Vol. 34, 2001, pp. 266-272.

[2] Maruyama, I. and Teramoto, A.," Impact of time-dependent thermal expansion coefficient on the early age volume changes in cement pastes," Cem. & Conr. Res., Vol. 41, 2011, pp. 380-391.

[3] Loser, B., Münch, B. and Lura, P.," A volumetric technique for measuring the coefficient of thermal expansion of hardening cement paste and mortar," Cem. & Conr. Res., Vol. 40, 2010, pp. 1138-1147.

[4] Granja, J. L. et al.," Hygrometric assessment of internal relative humidity in concrete: practical application issues," J. Adv. Concr. Technol., Vol. 12, 2014, pp. 250-265.

[5] Wyrzykowski, M. and Lura, P.," Effect of relative humidity decrease due to self-desiccation on the hydration kinetics of cement," Cem. & Conr. Res., Vol. 85, 2016, pp. 75-81.

[6] Morin, R., Haddad, G. and Aïtcin, P. C.," Crack free high performance concrete structures," Concr. Int., Vol. 24, 2002, pp. 43-48.